

Diffusion Barriers in the Squid Nerve Fiber

The axolemma and the Schwann layer

RAIMUNDO VILLEGAS, CARLO CAPUTO, and
LEOPOLDO VILLEGAS

From the Departamento de Biofísica, Instituto Venezolano de Investigaciones Científicas.
(I.V.I.C), Caracas, Venezuela

ABSTRACT The squid nerve barriers are formed by (a) the axolemma (membrane of the axon proper), a membrane 80 Å thick perforated by cylindrical pores 4.0 to 4.5 Å radius, and (b) the Schwann layer, constituted of numerous cells forming a layer one cell thick, crossed by 60 Å wide slit channels. If a molecule present in the axoplasm has to reach the extraneural space, it has to pass (a) the pores, and (b) the channels, in series, and the diffusion rate will depend on the effective diffusion areas per unit path length, $A_{pd}/\Delta x$ for the axolemma, and $A_{sd}/\Delta x$ for the Schwann layer. By addition, $A_{nd}/\Delta x$, the trans-neural effective area for diffusion per unit path length is obtained. The diffusion rates of C^{14} -ethylene glycol (2.2 Å radius), and C^{14} -glycerol (2.8 Å radius) were measured. The diffusion rate of H^3 -labeled water (1.5 Å radius) has been previously determined. The results expressed in terms of $A_{nd}/\Delta x$ (mean values \pm SD, referred to 1 cm² of nerve surface) are 5.3 ± 1.4 cm for water, 2.5 ± 0.4 cm for ethylene glycol, and 0.29 ± 0.03 cm for glycerol. Theoretical values for $A_{nd}/\Delta x$ of 2.5 and 0.83 cm for ethylene glycol and glycerol have been calculated. The agreement between the theoretical values for $A_{nd}/\Delta x$ and the experimental ones supports the diffusion barrier model described above.

Studies on the ultrastructure, the permeability to diffusion and filtration of water, and on molecular sieving in the squid giant nerve, have indicated the axolemma (membrane of the axon proper) as the excitable membrane of the physiologists. This conclusion followed the demonstration of the existence of 60 Å wide slit channels crossing the Schwann layer (1, 2), and of pores with an effective radius of 4.25 Å in the axolemma (2, 3). The value found for the effective pore radius in the axolemma indicates this membrane to be the only continuous barrier able to maintain the controlled ionic environment responsible for the normal functioning of the nerve. In view of the importance of

this conclusion, it seems necessary to provide additional experimental evidence of the validity of the observations on which it is based.

The present experiments deal with the measurements of the diffusion rates of C^{14} -labeled ethylene glycol and glycerol from the squid nerve. The rate of diffusion of H^3 -labeled water has been previously determined (2). The results obtained with these three molecules are used to calculate the geometrical and the effective diffusion areas per unit path and to evaluate the significance of the axolemma and the Schwann cell layer as diffusion barriers for graded size particles that do not show significant chemical interaction with these nerve constituents.

Although the observations and experiments reported in this paper deal exclusively with the squid nerve fiber, the results may give some insight into the functional significance of the submicroscopic organization of other biological systems.

EXPERIMENTAL METHOD

Procedure The giant nerve fiber from the first stellar nerve of the Venezuelan squid, *Doryteuthis plei*, was used. The axon diameter and the fiber length were measured and the fiber was handled as previously described (2). To make the data from different fibers comparable, results are referred to 1 cm^2 of nerve area. The single nerve fiber was transferred to a holder containing 10 ml of artificial sea water to which C^{14} -labeled ethylene glycol or glycerol had been added. The fiber was left in the radioactive solution for 80 minutes. After this period it was taken out, blotted gently with lens paper, and immediately soaked in a series of ten baths, each containing 2.5 ml of artificial non-radioactive sea water. The time of soaking in each bath was chosen in order to obtain an adequate number of counts in the baths. The length of time, in seconds, in each bath was measured by a chronometer with a precision of ± 1 second. It was estimated that the fiber remained in air less than 1 second as it was passed from one bath to the other. The fiber was left for 24 hours in a final bath to collect any remaining radioactivity in the nerve. Experiments were carried out at $22\text{--}24^\circ\text{C}$.

The results were accepted as valid when normal action potentials were evoked upon electrical stimulation before leaving the fiber in the 24 hour bath, a maneuver which was always executed less than 3 hours after the start of the experiment.

Composition of the Solutions Artificial sea water as described by Hodgkin and Katz (4) was used in all experiments. The radioactive solutions were prepared by adding to the artificial sea water (a) 10.2 millimols per liter of C^{14} -ethylene glycol (Experiments 10–16), or (b) 4.1 (Experiments 17–22) or 16.0 millimols per liter (Experiments 23–26) of C^{14} -glycerol. The specific activities of ethylene glycol and glycerol were 0.57 and 1.90 mc per millimol respectively. The concentrations used in all cases were so low that osmotic effects resulting from addition of the test molecules were negligible. The purity of the C^{14} -labeled solutes was tested by paper chromatography and paper radiochromatography.

Molecular Radii The molecular radii of 2.2 Å (2.24 ± 0.01 , mean \pm SE) for ethylene glycol and of 2.8 Å (2.77 ± 0.03) for glycerol, as obtained from constructed molecular models (3), are used in the present work.

Sample Analysis The concentration of C¹⁴-labeled solute in the artificial radioactive sea water and in each of the baths was determined by a liquid scintillation counter (Tri-Carb spectrometer, model 314). An aliquot of bath fluid was added to 10 ml of the following scintillation solution: 2,5-diphenyloxazole, 3.00 gm; 1,4-di-2-(5-phenyloxazolyl)-benzene, 0.10 gm; naphthalene, 50.00 gm; made up to 1000 ml with dioxane. Counting was performed at 6°C, with the pulse height discriminators set to receive pulses of 10 to 100 volts, and photomultiplier voltage of 1100 volts. The standard deviation of net counting was less than 2 per cent. The counting vials were discarded after each experiment to prevent effects caused by residual radioactivity.

RESULTS AND DISCUSSION

Experimental Effective Transneural Areas for Diffusion per Unit Path Length

The rate of efflux of C¹⁴-ethylene glycol was followed in seven single nerve fibers and the rate of efflux of C¹⁴-glycerol in ten single nerve fibers. Typical efflux curves are shown in Fig. 1. From the rate of efflux from the axoplasm, represented by the slope of the slowest phase of the curve, $A_{na}/\Delta x$, the effective transneural area for diffusion per unit path length (the Schwann layer and the axolemma considered together) between the axoplasm and the extracellular fluid is evaluated.

In the present experiments the difference between the slope of the slowest phase of the curves and that of the preceding phase was found to be larger than one order of magnitude. This allows one to consider the slope of the slowest phase equal to the rate constant of efflux for a single compartment (5). As shown in Fig. 2, direct analysis of extruded axoplasm of C¹⁴-glycerol-soaked nerves, at times corresponding to 0 and 1800 seconds in the efflux curve, has confirmed the correspondence of the slowest phase with the axonal compartment.¹

$A_{na}/\Delta x$ represents that ratio of the effective area to path length which is necessary to account for the observed diffusion rate on the basis of Fick's law:

$$dn/dt = -D_s (A_{na}/\Delta x) \Delta c_s \quad (1)$$

¹ In the red cell membrane of some species, a facilitated diffusion system which accelerates the movement of glycerol down a concentration gradient, has been described. Such a mechanism can be inhibited by copper (6, 7). $A_{na}/\Delta x$ for glycerol calculated from the slowest phase of the efflux curves of a group of copper-treated nerves, was found equal to the value reported in this paper for non copper-treated nerves. However, in the copper-treated nerve experiments it has become clear that there does exist a facilitated diffusion system for glycerol in the membrane of the endoneurium cells (8).

in which dn/dt is the diffusion rate from axoplasm to extracellular fluid, D_s is the free diffusion coefficient of the test solute in water, and Δc_s is the concentration difference. Values of $A_{nd}/\Delta x$ were computed from the efflux curve by means of the following equation:

$$A_{nd}/\Delta x = v \ln (c_s'/c_s'')/(\Delta t D_s) \quad (2)$$

which is an integrated solution of Equation 1; v is the volume of the axon, c_s' and c_s'' are the concentrations of test solute at time t' and t'' respectively, and Δt is the time interval ($t''-t'$). D_s has been assumed equal to the diffusion

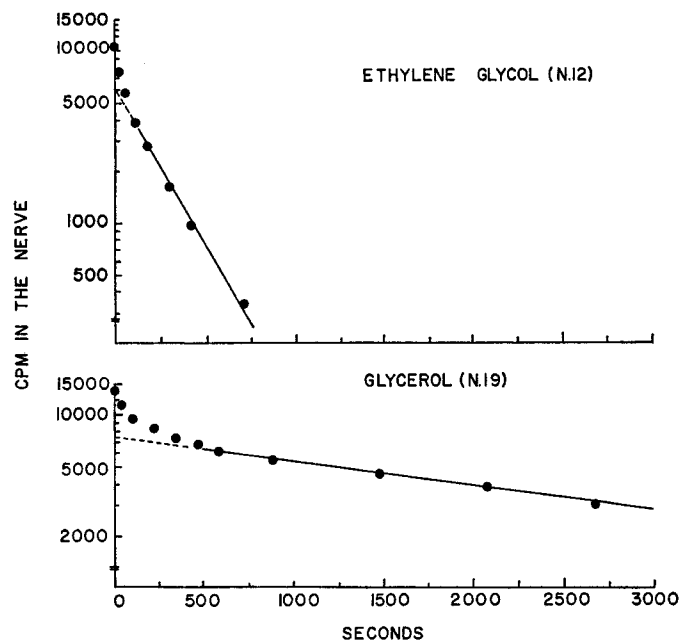


FIGURE 1. Efflux curves of C^{14} -ethylene glycol (nerve 12) and C^{14} -glycerol (nerve 19) from giant nerve fibers of the squid. The slope of the slower phase of each of the experimental curves is considered to represent the rate of efflux of the respective C^{14} -labeled molecule from the axoplasm. Typical efflux curve of H^3 -water has been previously published (2).

coefficient of the test solutes in aqueous solution which are equal to 1.09×10^{-5} $\text{cm}^2/\text{sec.}$ for ethylene glycol and 0.89×10^{-5} $\text{cm}^2/\text{sec.}$ for glycerol (9), at the experimental concentrations.

$A_{nd}/\Delta x$ is found to be 2.5 ± 0.4 cm per cm^2 of nerve area for ethylene glycol, and 0.29 ± 0.03 cm per cm^2 of area for glycerol (see Tables I and II). For water a value of 5.3 ± 1.4 cm per cm^2 of nerve area has been found (2). When the values of $A_{nd}/\Delta x$ for water, ethylene glycol, and glycerol are compared, it can be observed that the transneural effective area for diffusion per unit path decreases with increasing molecular radius (see Table I). No similar relation is found between the permeability of the nerve to water,

ethylene glycol, and glycerol and their respective oil-water partition coefficients. A similar conclusion was reached and discussed in a previous work (3) in which the sieving properties of the squid nerve to water and six non-

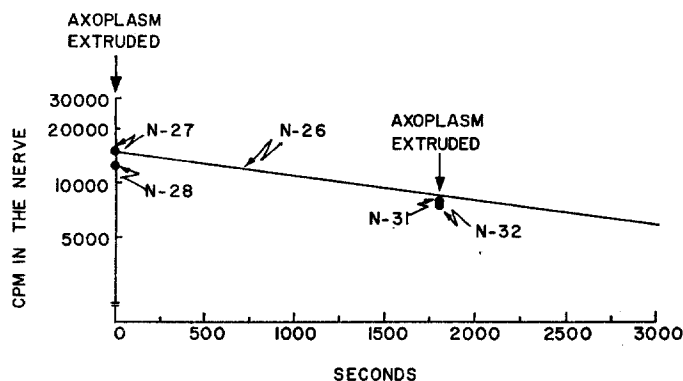


FIGURE 2. Identification of the slowest phase in the C^{14} -glycerol curve with the efflux from the axon compartment. The continuous line corresponds to the slowest phase from nerve 26. The solid circles represent the C^{14} -glycerol contents for volumes of axoplasm from nerves 27, 28, 31, and 32, equal to that from nerve 26 ($3.5 \times 10^{-3} \text{ cm}^3$). The content of C^{14} -glycerol in the axoplasm was measured at times corresponding to zero in the efflux curve of nerves 27 and 28, and to 1800 seconds in the efflux curve of nerves 31 and 32. The diameters of the axons in 10^{-4} cm were: 312, 320, 316, 328, and 312, for nerves 26, 27, 28, 31, and 32, respectively. The axoplasm was extruded and weighed as described in a previous paper (2). The analysis of the samples for the determination of the C^{14} -glycerol content was carried out as described in the text for radioactive baths. We are indebted to Dr. Maximo Gimenez for his assistance in these experiments.

electrolytes (including ethylene glycol and glycerol) were studied. The passage through the nerve barriers of the water and the non-electrolyte molecules studied seems to be related to the molecular sizes.

The Theoretical Axolemmal, Schwann Layer, and Transneuronal Areas for Diffusion per Unit Path Length

As shown in Fig. 3 the nerve barriers are considered as being formed by (a) the axolemma, a membrane 80 \AA thick perforated by cylindrical pores 4.25

TABLE I
DIFFUSION DATA OF THE TEST MOLECULES

Molecule	Radius	Diffusion coefficient (23°C)	Olive oil/water partition coefficient	$(A_{nd}/\Delta x)^*$
	\AA	$10^{-8} \text{ cm}^2/\text{sec.}$	10^{-1}	cm
Water	1.5 (10)	2.65 (11)	0.00	5.3 ± 1.4 (2)
Ethylene glycol	2.2 (3)	1.09 (9)	0.47 (12)	2.5 ± 0.4
Glycerol	2.8 (3)	0.89 (9)	0.07 (12)	0.29 ± 0.03

* Values (\pm SD) for $A_{nd}/\Delta x$ are referred to 1 cm^2 of nerve surface. Numbers in parentheses are references.

Å in radius (3), and (b) the Schwann layer, made up of numerous Schwann cells forming a layer one cell thick (13) crossed by 60 Å wide slit channels (1, 2), connecting the extracellular space with the 80 Å wide axolemma-Schwann cell space. The extracellular nature of the Schwann channel lumina has been recently confirmed (13).

If a molecule present in the axoplasm has to diffuse through to the connective tissue, it has to pass (a) the pores, and (b) the channels, in series, and the diffusion rate will depend on the effective diffusion areas per unit path length, $A_{pd}/\Delta x$ for the pore, and A_{cd} for the channel. In Fick's equation,

TABLE II
TRANSNEURAL EFFECTIVE AREAS PER UNIT PATH
LENGTH FOR THE DIFFUSION OF C¹⁴-LABELED ETHYLENE
GLYCOL AND GLYCEROL
Temperature, 22–24°C.

	Nerve No.	Radius	Area	($A_{nd}/\Delta x$)*
		10^{-4} cm	cm ²	cm
Ethylene glycol	10	137	0.18	2.3
	11	130	0.18	2.2
	12	144	0.20	2.8
	13	135	0.31	2.2
	14	156	0.44	3.2
	15	173	0.41	2.3
	16	159	0.44	2.6
Mean ± SD				2.5±0.4
Glycerol	17	154	0.20	0.30
	18	149	0.25	0.24
	19	149	0.28	0.31
	20	151	0.30	0.27
	21	187	0.42	0.32
	22	151	0.33	0.32
	23	144	0.19	0.27
	24	156	0.37	0.28
	25	168	0.36	0.31
	26	156	0.44	0.27
Mean ± SD				0.29±0.03

* Values for $A_{nd}/\Delta x$ are referred to 1 cm² of nerve surface.

$A/\Delta x$ has the character of a conductance, and may be treated as such. Therefore, by addition, a theoretical $A_{nd}/\Delta x$ may be calculated. Some investigators have explained their experimental results in other tissues in terms of the possible existence of a similar double barrier arrangement (14–17).

$A_{pd}/\Delta x$, the effective area per unit path for diffusion of any molecule of radius r_x passing through a membrane, *i.e.* the axolemma perforated by

cylindrical pores, is given by Renkin's (18) equation 11:

$$\begin{aligned} \frac{A_{pd}}{\Delta x} &= \frac{A_p}{\Delta x} \left(1 - \frac{r_x}{r_p}\right)^2 \left[1 - 2.104 \left(\frac{r_x}{r_p}\right) + 2.09 \left(\frac{r_x}{r_p}\right)^3 - 0.95 \left(\frac{r_x}{r_p}\right)^5\right] \\ &= \frac{A_p}{\Delta x} f\left(\frac{r_x}{r_p}\right) \end{aligned} \quad (3)$$

in which $A_p/\Delta x$ is the geometrical pore area per unit path, and r_p the pore radius. In this equation $(1 - r_x/r_p)^2$ represents the steric factor restricting the entrance of the molecule into the pore, and the bracketed expression the viscous drag at the wall once the molecule has entered the pore.

To determine $A_{cd}/\Delta x$, the effective area for diffusion per unit path of any molecule of radius r_x passing through a barrier crossed by slit channels as the Schwann layer, the following equation is used:

$$\begin{aligned} \frac{A_{cd}}{\Delta x} &= \frac{A_c}{\Delta x} \left(1 - \frac{r_x}{0.5c}\right) \left[1 - 1.004 \left(\frac{r_x}{0.5c}\right) + 0.42 \left(\frac{r_x}{0.5c}\right)^3 - 0.17 \left(\frac{r_x}{0.5c}\right)^5\right] \\ &= \frac{A_c}{\Delta x} f\left(\frac{r_x}{0.5c}\right) \end{aligned} \quad (4)$$

in which $A_c/\Delta x$ is the geometrical slit channel area per unit path, and c is the 60 Å channel width. The steric factor at the entrance of the channel is given by $(1 - r_x/0.5c)$; the viscous drag at the walls by the bracketed expression which is equal to the expression for this factor derived by Faxen (19).

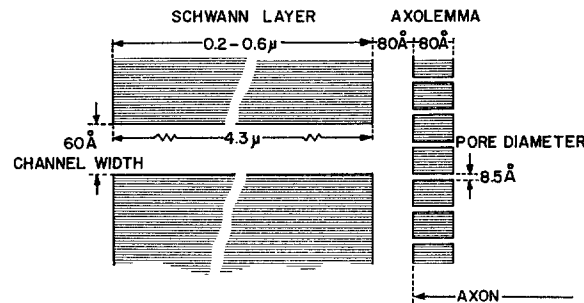


FIGURE 3. Arrangement of the barriers, axolemma, and Schwann layer, between the axoplasm and the extracellular fluid for theoretical analysis of the data. A labeled molecule in the axoplasm has to pass the pores in the axolemma, and the channels in the Schwann layer to reach the extraneural space. The dimensions in the figure are those obtained from the electron microscopy observations (1, 2), the water diffusion and filtration permeability studies (2), and the measurements of the sieving properties of the axolemma to non-electrolytes (3).

An estimate of $A_{nd}/\Delta x$, the transneural area for diffusion per unit path (the axolemma and the Schwann cell layer considered together) may be calculated for a molecule by adding as conductances in series, the values ob-

tained for $A_{pd}/\Delta x$ and $A_{cd}/\Delta x$ from Equations 3 and 4:

$$\frac{A_{nd}}{\Delta x} = \left[\frac{1}{(A_{pd}/\Delta x)} + \frac{1}{(A_{cd}/\Delta x)} \right]^{-1} \quad (5)$$

$A_{pd}/\Delta x$ for ethylene glycol or glycerol in the axolemma may be obtained from Equation 3. The values of r_x , and r_p are known. $A_p/\Delta x$ may be calculated from $(A_{pd}/\Delta x)_w$, the subscript w denotes water, by means of the expression: $A_p/\Delta x = (A_{pd}/\Delta x)_w/f (r_w/r_p)$. Substituting 13.6 cm per cm² of axolemma (3) for $(A_{pd}/\Delta x)_w$, $A_p/\Delta x$ is found to equal 90.7 cm per cm² of axolemma. Upon introducing the values of $A_p/\Delta x$, r_p , and r_x for a given test molecule in Equation 3, its corresponding $A_{pd}/\Delta x$ is obtained. For ethylene glycol and glycerol $A_{pd}/\Delta x$ is calculated to be 3.5 and 1.0 cm per cm² of axolemma, respectively.

$A_{cd}/\Delta x$ may be calculated for ethylene glycol or glycerol in the Schwann layer from Equation 4. $A_c/\Delta x$ is calculated by means of Equations 4 and 5, from values already known for water. Upon introducing into Equation 5 the values of $(A_{pd}/\Delta x)_w$ equal to 13.6 cm per cm² of axolemma, and $(A_{nd}/\Delta x)_w$

TABLE III
EFFECTIVE AREAS PER UNIT PATH LENGTH FOR
THE DIFFUSION OF WATER, ETHYLENE GLYCOL, AND
GLYCEROL IN THE SQUID NERVE FIBER

Molecular radius	$A_{pd}/\Delta x$ (axolemma)	$A_{cd}/\Delta x$ (Schwann layer)	$A_{nd}/\Delta x$ (transneural)	
			Theoretical	Experimental*
<i>in cm per cm² of nerve area</i>				
Water 1.5 Å	13.6	8.7	—	5.3±1.4
Ethylene glycol 2.2 Å	3.5	8.3	2.5	2.5±0.4
Glycerol 2.8 Å	1.0	7.9	0.83	0.29±0.03

* Mean value ± the standard deviation.

equal to 5.3 cm per cm² of nerve surface, $(A_{cd}/\Delta x)_w$ is found equal to 8.7 cm per cm² of Schwann layer surface. $A_c/\Delta x$ is then calculated from Equation 4 as follows: $A_c/\Delta x = (A_{cd}/\Delta x)_w/f (r_w \cdot 0.5c) = 9.6$ cm per cm² of Schwann layer surface. Having determined the values of $A_c/\Delta x$, Equation 4 may be evaluated for any test solute introducing the corresponding values of r_x . $A_{cd}/\Delta x$ for ethylene glycol and glycerol is found equal to 8.3 and 7.9 cm per cm² of Schwann layer surface, respectively.

The theoretical $A_{nd}/\Delta x$ for ethylene glycol or glycerol may be calculated by introducing the values obtained for $A_{pd}/\Delta x$ and $A_{cd}/\Delta x$ corresponding to ethylene glycol and glycerol in Equation 5. Theoretical values for $A_{nd}/\Delta x$ are 2.5 and 0.83 cm per cm² of nerve area for ethylene glycol and glycerol, respectively. These calculated values are in good agreement with the values

found experimentally of 2.5 ± 0.4 cm per cm^2 of nerve area for ethylene glycol, and of 0.29 ± 0.03 cm per cm^2 of area for glycerol. In Table III the values for the effective areas for diffusion per unit path length for water, ethylene glycol, and glycerol in the axolemma, $(A_{pd}/\Delta x)$, in the Schwann layer, $(A_{cd}/\Delta x)$, and in the axolemma and the Schwann layer considered together, $(A_{nd}/\Delta x)$, are presented. The agreement of the theoretical values for $A_{nd}/\Delta x$ with the experimental ones supports the diffusion barrier arrangement shown in Fig. 3, from which the theoretical values were calculated. The slight differences between the experimental results and the theoretical values may be related to the inherent errors in the molecular radii used for the test substances and to the use of the free diffusion coefficients of the test solutes in the computation of the experimental values of $A_{nd}/\Delta x$. The close relation between the radii of the molecules and the radius of the diffusion paths in the axolemma makes critical the values used for these parameters.

The Significance of the Schwann Layer and the Axolemma as Diffusion Barriers

It has been previously calculated that there are 1.3×10^{10} pores per cm^2 of axolemma, occupying 7.6×10^{-5} cm^2 per cm^2 of axolemma (3). The area occupied by the slit channels may be estimated from $A_c/\Delta x = 9.6$ cm and $\Delta x = 4.3 \mu$ (2), to equal 4.1×10^{-3} cm^2 per cm^2 of Schwann layer surface. The area occupied by the channels in 1 cm^2 of Schwann layer surface is some 54 times larger than the one occupied by the pores in 1 cm^2 of axolemma. The channels are about 540 times longer than the pores, if the latter are considered to have a length equal to 80 Å, the axolemma thickness. The restriction offered by each barrier to diffusion, $(A/\Delta x)^{-1}$, is dependent on both the area and the length of the pathways crossing the barrier. Thus, the restriction to the diffusion of the test molecules offered by the channels crossing the Schwann layer is mainly due to their length, and that offered by the pores in the axolemma to their small radius. This is schematically shown in Fig. 3.

The value of 9.6 cm for the ratio $A_c/\Delta x$ (geometrical area per unit path length for the Schwann layer) is 9.4 times smaller than $A_p/\Delta x$ (geometrical area per unit path length for the axolemma). The width of the channels crossing the Schwann layer, 20 times larger than the diameter of the water molecule and almost 10 times the diameter of the glycerol molecule, makes the values for $A_{cd}/\Delta x$ for diffusion of water, ethylene glycol, and glycerol across the Schwann layer closely similar to $A_c/\Delta x$. Thus the effective ratio for water is 8.7 cm, for ethylene glycol, 8.3 cm, and for glycerol, 7.9 cm. On the contrary, although the axolemma has a larger geometrical area to path length ratio than the Schwann layer, it possesses narrow pores which allow it to distinguish small particles critically by size; thus $A_p/\Delta x$ which equals 90.5 cm, has effective values, $A_{pd}/\Delta x$, of 13.6 cm for the diffusion of water, 3.5 cm for ethylene glycol, and 1.0 cm for the passage of glycerol. Thus the resistance to diffusion for glycerol is 7.9 times larger at the axolemma than

at the Schwann layer. This ratio should become larger for particles bigger than glycerol which has a molecular radius of 2.8 Å.

Staverman (20, 21) has indicated that penetration of membranes by solute relative to water can be expressed by the reflection coefficient, σ . The limiting values for this coefficient are: (a) $\sigma = 1$ in the case of an ideally selective membrane, and (b) $\sigma = 0$ when solute and solvent (water) pass across the membrane at an equal rate. Durbin (16) has demonstrated experimentally the relation between σ and the ratio of the filtration areas for solute and water. The values of σ , previously determined in the axolemma of the squid nerve, have been found to be 0.72 for ethylene glycol and 0.96 for glycerol (3). From the present diffusion data a similar coefficient σ' may be calculated from Kedem and Katchalsky's Equations 4-7 and 4-11 (22), as follows:—

$$\begin{aligned}\sigma' &= 1 - (A_{pd}/\Delta x)_s / (A_{pd}/\Delta x)_w \text{ for the axolemma} \\ \sigma' &= 1 - (A_{cd}/\Delta x)_s / (A_{cd}/\Delta x)_w \text{ for the Schwann layer}\end{aligned}$$

in which the subscripts s and w refer to solute and water, respectively. Values for σ' of 0.74 for ethylene glycol and 0.93 for glycerol in the axolemma, agree with the filtration values for the same membrane and show the high degree of impermeability of the axolemma for molecules as small as 2.2 Å, and its ability to distinguish small particles by size. On the contrary, σ' values for the Schwann layer of 0.05 and 0.09 for ethylene glycol and glycerol, indicate the low degree of selectivity of the Schwann layer. Thus, the axolemma appears to be the only continuous barrier able to distinguish small particles critically by size and to maintain the concentration differences between axoplasm and the outside, necessary for the normal functioning of the nerve.

The findings herein described and discussed support the previously proposed (3) function of the axolemma (membrane of the axon proper) as the excitable membrane studied by the physiologists. This conclusion is independent of and compatible with any of the hypotheses used to explain the ion transport processes in the nerve (23-25). Moreover, the electrical characteristics of the squid nerve excitable membrane, determined by Cole and Curtis (26, 27), also agree with the proposed identification of the axolemma with the excitable membrane. The excitable membrane was found by these authors to have an average capacity of 1.1 μf per cm^2 and a resistance of the order of 1000 ohm cm^2 in resting state. The capacity of 1.1 μf per cm^2 leads to an estimate of the excitable membrane thickness between 50 to 150 Å, in accord with the electron microscopy measurements of 80 Å for the axolemma thickness (1, 2). The resistance might be related to the area occupied by the pores crossing the axolemma. Taking the pore length as 80 Å (3), and assuming with Nevis (28) the specific resistivity of their content to lie between the value for sea water equal to 20.5 ohm cm (29), and that of equilibrium water equal

to 0.5×10^6 ohm cm (30), an area of 2×10^{-8} to 5×10^{-4} cm² of membrane is calculated to be occupied by pores. The value of 7.6×10^{-5} cm² (3) which has been found from analysis of water and non-electrolyte permeability to be occupied by pores in 1 cm² of axolemma falls within this range.

Our thanks are due to Dr. L. G. Longworth for allowing us to use his data on the diffusion coefficient of the test molecules; to Dr. Karl Gaede and Dr. Providencia Rodriguez for the paper chromatographic and radiochromatographic analysis of the C¹⁴-labeled molecules; to Dr. Guillermo Whitembury and Dr. Fidel Alsina for valuable discussions of the manuscript. The technical assistance of Miss Laura Sananes is gratefully acknowledged.

Received for publication, April 12, 1962.

BIBLIOGRAPHY

1. VILLEGAS, G. M., and VILLEGAS, R., *J. Ultrastructure Research*, 1960, **3**, 362.
2. VILLEGAS, R., and VILLEGAS, G. M., *J. Gen. Physiol.*, 1960, **43**, No. 5, suppl., 73.
3. VILLEGAS, R., and BARNOLA, F. V., *J. Gen. Physiol.*, 1961, **44**, 963.
4. HODGKIN, A. L., and KATZ, B., *J. Physiol.*, 1949, **108**, 37.
5. DAINTY, J., and KRNJEVIC, K., *J. Physiol.*, 1955, **128**, 489.
6. LE FEVRE, P. G., *J. Gen. Physiol.*, 1948, **31**, 505.
7. STEIN, W. D., *Nature*, 1961, **191**, 352.
8. VILLEGAS, R., and VILLEGAS, G. M., *Biochim. et Biophysica Acta*, 1962, **60**, 202.
9. LONGSWORTH, L. G., personal communication.
10. MORGAN, J. R., and WARREN, B. E., *J. Chem. Physics*, 1938, **6**, 666.
11. WANG, J. H., ROBINSON, C. V., and EDELMAN, I. S., *J. Am. Chem. Soc.*, 1953, **75**, 466.
12. COLLANDER, R., and BÄRLUND, H., *Acta Bot. Fenn.*, 1933, **11**, 5.
13. VILLEGAS, G. M., and VILLEGAS, R., *J. Ultrastructure Research*, in press.
14. LEAF, A., *J. Cell. and Comp. Physiol.*, 1959, **54**, 103.
15. CURRAN, P. F., *J. Gen. Physiol.*, 1960, **43**, 1137.
16. DURBIN, R. P., *J. Gen. Physiol.*, 1961, **44**, 315.
17. WHITTEMBURY, G., *J. Gen. Physiol.*, 1962, **46**, 117.
18. RENKIN, E. M., *J. Gen. Physiol.*, 1954, **38**, 225.
19. FAXEN, H., *Ann. Physik.*, 1922, **68**, 89.
20. STAVERMAN, A. J., *Rec. trav. chim. Pays-bas*, 1951, **70**, 344.
21. STAVERMAN, A. J., *Rec. trav. chim. Pays-bas*, 1952, **72**, 623.
22. KEDEM, O., and KATCHALSKY, A., *J. Gen. Physiol.*, 1961, **45**, 143.
23. HODGKIN, A. L., and KEYNES, R. D., *J. Physiol.*, 1955, **128**, 28.
24. HODGKIN, A. L., *Proc. Roy. Soc. London, Series B*, 1957, **148**, 1.
25. MULLINS, L. J., *Ann. New York Acad. Sc.*, 1961, **94**, 390.
26. CURTIS, H. J., and COLE, K. S., *J. Gen. Physiol.*, 1938, **21**, 757.
27. COLE, K. S., and CURTIS, H. J., *J. Gen. Physiol.*, 1939, **22**, 649.
28. NEVIS, A. H., *J. Gen. Physiol.*, 1958, **41**, 927.
29. COLE, K. S., and CURTIS, H. J., *J. Gen. Physiol.*, 1939, **22**, 671.
30. KOTÜM, G., and BOCKRIS, J. O'M., *Textbook of Electrochemistry*, Amsterdam, Elsevier Publishing Company, Inc., 1951, **2**, 566.